MODELLING OF FULL WAVEFORM ACOUSTIC LOGS IN SOFT MARINE SEDIMENTS

by

C.H. Cheng, R.H. Wilkens and J.A. Meredith

Earth Resources Laboratory
Department of Earth, Atmospheric, and Planetary Sciences
Massachusetts Institute of Technology
Cambridge, MA 02139

ABSTRACT

Full waveform acoustic logs obtained from the Deep Sea Drilling Project (DSDP) were modelled using synthetic full waveform acoustic logs. These synthetic logs were calculated using the discrete wavenumber method. The model is that of a fluid-filled borehole with a rigid logging tool in the center. Results from the modelling indicate that V_p, V_s, and V_f along with P wave attenuation $(1/Q_p)$ are the primary controls on the full waveform acoustic logs of these soft sediments. S-wave attenuation $(1/Q_s)$ does not play a major role because the S-wave velocities (V_s) of these fluid-saturated marine oozes are lower than the borehole fluid velocity (V_f), thus there is no refracted S-wave or pseudo-Rayleigh wave. However, the formation S-wave velocity does affect the amplitude of the observed P-wave train. Density variations by themselves have almost no discernible effect on the synthetics although in practice a change in density often is concurrent with a change in lithology and formation velocities. Matching the synthetic full waveform acoustic logs to those obtained during Leg 95 of the DSDP was formally done by a least squares linearized iteration inversion procedure. Only the P wavetrain and its associated leaky modes were taken into account. The forward model used in the inversion was a P-wave train generated by the branch cut integral method. Stable results in V_s and Q_p were obtained. Variations in the velocity and attenuation from the inversion correlates with sedimentary units delineated from conventional logs and lithologic units identified by shipboard stratigraphers for the Baltimore Canyon Trough area. Full waveform logs, in combination with conventional logs, help to identify changes in the physical properties of these sediments as a result of the diagenesis of biogenic silica and calcium carbonate.

INTRODUCTION

Very little is known about the *in situ* acoustic properties of soft marine sediments. These materials, which generally constitute the upper 300 to 500 meters of the sea floor, are generally represented in seismic modelling studies as some uniform layer with

homogeneous values of velocity and attenuation. Clearly this is not the case in the actual environment, as this is the zone in which the sediments transform from high porosity oozes, with properties close to that of water, to sedimentary rocks, whose properties are known from continental field studies and laboratory experimentation. In particular, there have not been any *in situ* measurements of shear wave velocity in these sediments. During Leg 95 of the Deep Sea Drilling Project (DSDP), in addition to a regular set of logs, full waveform acoustic logs were obtained using the Schlumberger SLS-TA tool. Because of the low shear wave velocity in these sediments, there are no observable refracted shear wave arrivals. However, since the V_p/V_s ratio, or equivalently, the Poisson's ratio, affects the amplitude of the P-wave train (Cheng and Toksöz, 1981), information about the shear wave velocity of the formation can be obtained from the full waveform logs.

In this paper, we first demonstrate the effects of different formation properties on the full waveform logs by synthetic examples. We then analyze the DSDP Leg 95 full waveform data to obtain formation shear wave velocities and P-wave attenuation using a nonlinear least squares inversion technique based on the branch cut integral representation of the P-wave train (Tsang and Rader, 1979). The results are then combined with other logs and core data for the interpretation of the changes in lithology and physical properties of these sediments in terms of diagenesis of biogenic silica and calcium carbonate.

RESULTS OF SYNTHETIC MODELS

An instructive tool in the better understanding of full waveform acoustic logs in marine sediments is the use of the forward model of the entire wavetrain. By holding all but one of the input variables constant, it is possible to gain some qualitative sense of the relative importance of the differing parameters such as velocity, density and attenuation.

Forward Model Description

To generate the synthetic full waveform acoustic logs, we first calculated the instantaneous pressure response of a fluid-filled borehole in a homogeneous formation to a point source. A rigid logging tool is placed in the middle of the borehole. The technique of discrete wavenumber integration (Bouchon and Aki, 1977; Cheng and Toksöz, 1981) was used to calculate the formation pressure response. Convolution of the formation pressure response with a source-time function then follows. A typical synthetic source was given by Tsang and Rader (1979). This source is a decaying sinusoid, with the property that the center frequency and bandwidth can be adjusted independently.

With this forward synthetic microseismogram model, we can systematically inves-

tigate the effects of different formation properties on the observed full waveform microseismograms. In the following paragraphs, we describe the results of varying the Poisson's ratio (equivalent to varying the V_p/V_s ratio), and the formation P- and S-wave attenuation. We will focus our discussion on formations with properties similar to those found in ocean bottom soft sediments. The source chosen was a Tsang and Rader (1979) source with a center frequency of 11.5 kHz and an α of 0.4.

Figure 1 shows the effect of varying Poisson's ratio while keeping compressional wave velocity constant at 1.85 km/sec and Q values constant. Poisson's ratio changes from 0.32 in the top microseismogram to 0.44 in the bottom microseismogram. As pointed out by Cheng and Toksöz (1981) and Paillet and Cheng (1986), the P wave amplitude increases with increasing Poisson's ratio. This is related to the fact that less and less energy is converted into shear waves when the S-wave velocity is low (Stephen et al., 1985). In these particular examples, it is the Airy phase associated with the P leaky mode (arriving at about 1.75 msec) that shows the largest amplitude increase as the S-wave velocity decreases and Poisson's ratio increases. The first arriving P-wave pulse shows a slight decrease with increasing Poisson's ratio.

Figure 2 shows the effect of increasing formation P-wave attenuation. Formation Q_p decreases from 100 to 50 to 35 in these three traces (top to bottom). Both the first arriving P-wave and the Airy phase of the P leaky mode show decreasing amplitude with increasing attenuation, although the effect is more pronounced for the first arrival. This is because the P leaky mode is a guided wave whose properties are influenced by both the formation and borehole fluid properties. With the borehole fluid attenuation held constant, the relative effect of formation P-wave attenuation on the P leaky mode is less than the first arriving P wave.

Figure 3 shows the effect of increasing Q_s, or decreasing formation S-wave attenuation, on the microseismograms. From top to bottom, Q_s increases from 10 to 20 to 50. Despite an 80% decrease in attenuation, the microseismograms look quite similar, with only a slight increase in amplitude. This can be understood by the fact that there is no refracted shear wave energy in these microseismograms, nor is there any shear normal mode/pseudo-Rayleigh wave energy. The shear wave contribution comes in indirectly through the P wave and P leaky mode, and it is the shear wave velocity, not attenuation, that is influencing the P mode amplitudes.

With these synthetic examples, we can see that the two factors with the most influence on the full waveform acoustic log microseismograms in soft sediments are the V_p/V_s ratio and Q_p. Given V_p from conventional logs, one can then try to estimate V_s and Q_p from the full waveform data. One way to do it is the non-linear least squares inversion technique. In the next section, we will describe some results obtained for data collected from DSDP Leg 95 using this technique.

APPLICATIONS TO DATA — BALTIMORE CANYON TROUGH

Description of Sites 612 and 613

In the Fall of 1983 the drilling ship Glomar Challenger, under the control of the Deep Sea Drilling Project, drilled several boreholes on the continental slope off the coast of New Jersey (Leg 95 Scientific Party, 1984). Two of the sites were logged during the cruise, one in approximately 1400m of water (Site 612) and the other at 2333m depth (Site 613). Drilling and coring at both locations reached depths of around 600m below the seafloor (BSF). Both sites were located near U.S.G.S. multichannel seismic line 25 (Figure 4) and were intended to aid in the interpretation of the regional seismostratigraphy of the eastern U.S. continental margin.

Shipboard sedimentologists identified five major lithologic units at Site 612 based on examination of the cored material. At Site 613 the drilling was terminated near the base of Unit III and did not penetrate into the older units cored at Site 612. The sediments ranged in age from Upper Pleistocene to Upper Cretaceous and contained several significant hiatuses. Unit I is a Pleistocene to Upper Miocene section of terrigenous muds and glauconitic sands. Below that is a sequence of Lower Oligocene to Lower Eocene nannofossil oozes and chalks (Unit II) and Lower Eocene chalks and porcellanites (Unit III). Units IV and V consisted of Cretaceous shales and marly chalks.

Logging was carried out at each site by Schlumberger, under contract to the DSDP. Full waveform acoustic logs were collected at each site using the SLS-TA sonde. Results of conventional borehole compensated P-wave velocity (BHC), resistivity (DIL - corrected to formation factor using pore fluid conductivity), and gamma ray (GR) logs from Site 613 are shown in Figure 5. The drill pipe was left in the hole to a depth of approximately 100m to prevent collapse of the borehole in the uppermost, unconsolidated section.

Of particular interest to this study is the transition from the weakly cemented and only slightly altered oozes and chalks of Unit II to the chalks and porcellanites of Unit III. Over a very short interval (440-444m BSF at Site 613) all of the biogenic silica components of the sediment are seen in petrographic samples to dissolve and reprecipitate as a silica cement and pore filling phase represented by micron size silica lepispheres. At this point in the sedimentary column velocity increases, porosity decreases, and yet the chemical composition of the material remains the same (Wilkens et al., 1986).

Inversion Technique

Inversion of the full waveform acoustic logs recorded at Site 613 reveal the changes in shear wave velocity and compressional wave attenuation attendant to this diagenetic transformation. The problem of determining V_s and Q_p from the full waveform data is

addressed using a standard non-linear iterative least squares inversion technique in the frequency domain. In order to avoid the problem of unknown source function, it was decided to use the amplitude ratio of the frequency spectra at two receiver distances (8 and 10 ft.). In order to minimize the contribution of noise in the spectral ratio, only the ratio in the frequency band between 7.5 and 15 kHz is used. This band corresponds to the peak energies in the spectra. For the forward model used in the inversion the branch cut integration technique of Tsang and Rader (1979) has been chosen to model the P-wave train. By retaining successively higher terms in the ray expansion of Tsang and Rader (1979), the modal behavior of the P wave and the P leaky mode, including the Airy phase, can be modelled (Paillet and Cheng, 1986). This is a much faster technique than the full discrete wavenumber integration (which includes all other arrivals) used in the previous section for forward modelling. Since the data were collected in soft sediments, there are no refracted shear wave and psuedo-Rayleigh wave arrivals, and the Stoneley wave arrival in the waveform frequency band is very weak. Thus it can be safely assumed that most of the energy in the data is P wave and P leaky mode energy, and can be modelled by the branch cut integral of Tsang and Rader (1979). The effect of the tool in the borehole is approximated by using a borehole radius slightly larger than the width of the fluid annulus between the borehole and the tool (Cheng and Toksöz, 1981). Attenuation is introduced by the use of complex frequencies (Cheng et al., 1982). The inversion is weighted towards the shear wave velocity rather than Q_p. The spectral ratio data is weighted by the inverse of the frequency. Q_f, the borehole fluid attenuation, is inverted for a few depths together with V_s and Q_p to find a stable value which is then held constant for the rest of the data set. To test the inversion algorithm, synthetic data were generated using the discrete wavenumber summation technique (Cheng and Toksöz, 1981). The P-wave trains from two different receiver offsets are then windowed and their spectral ratio inverted for V_s, Q_p and Q_f. The results show better than one percent convergence for V_s and Q_p but much larger error for Q_f. At this time the inversion technique is not very sensitive to Q_f, but differences in Q_f are more important to the total amplitude of the signal than to the relative amplitudes of the different phases, and thus will not seriously affect the determinations of Q_p and V_s.

Results of Inversion

Results of the inversion for thirteen waveforms from differing depths are presented in Table 1.

A comparison of a waveform recorded at 200m BSF to a forward model produced using the inversion results is shown in Figure 6. The general characteristics of both the real and synthetic waveforms are similar. Differences in detail, particularly of the coda, are attributable to differences between the actual source characteristics and the function used to simulate the source in the forward model, the fact that the logging tool was not taken into account, and inhomogeneities in the formation. Any large changes in either Q_p or V_s, as illustrated in the previous section, would greatly alter the overall

Table 1: Site 613 Inversion Results

DEPTH mBSF	V_p (km/sec)	V_s (km/sec)	Q_p
200	1.75	0.70	75
270	1.75	0.75	35
282	1.76	0.75	25
402	1.91	0.88	20
417	1.85	0.84	13
435	1.90	0.88	11
456	1.95	0.88	10
472	2.00	0.81	15
487	2.05	0.65	12
502	2.05	0.75	17
520	2.00	0.76	11
539	2.10	0.66	12
560	2.10	0.87	10

aspect of the synthetic waveform.

Shear wave velocities are plotted versus compressional wave velocities in Figure 7. In general, within the section used for wavform inversion, there is an increase in V_p with depth (Figure 5) so that V_p/V_s ratios from left to right are indicative of changes with depth in the section. In terms of this ratio there appears to be some consistency in Units I and II and considerable variability in Unit III. Unit I V_p/V_s ratios are near 2.5, while Unit II values are near 2.5 at the top of the section and closer to 2.2 at the bottom. The uppermost measurement in Unit III is also close to 2.5, but values within the unit are variable, with V_p/V_s exceeding 3.0 for two of the inversion results. Most of the variation in V_p/V_s within Unit III is due to changes in V_s. It should also be noted that the "goodness" of fit to the data is somewhat degraded in the uppermost unit sampled and increases with depth. This may be attributed to the increased consolidation with depth leading to a more homogeneous formation.

While V_p/V_s ratios are somewhat variable, there appears to be much more consistency in values of Q_p. Compressional wave velocity is plotted versus Q_p in Figure 8. The general trend is for decreasing Q_p with increasing V_p (or depth). As with the velocity ratios, the uppermost measurement of Unit II appears more like Unit I. Q_p values lower in Unit II are much the same as in Unit III and given the various assumptions in the inversion, can be seen as essentially the same. Goldberg et al. (1985) calculated

similar values of Q_p in their examination of Site 613 waveforms. It is interesting to note that laboratory measurements of Q_p and Q_s in deep sea sediments with slightly greater compressional wave velocities are in agreement with the results of the inversions for Q_p and suggest that Q_p and Q_s are approximately equal.

Analysis of Data

Before discussing the implications of the data or the possible nature of the causes for variation in the inversion results, two qualifications must be kept in mind. The first is the preliminary nature of the inversion technique itself. It is satisfying that inversion results reflect values similar to laboratory studies; however, it is expected that the actual numbers may change somewhat as the technique evolves. The trends in the data, such as the decrease in Q_p with depth, are likely to remain unchanged and can be discussed with greater confidence. A second problem, related to understanding of the meaning of the results, is the fact that the data, while consistent between Sites 613 and 612, are essentially from one environment. It is not possible to adequately discriminate between factors related purely to compaction with depth and those which might be related to compositional changes. This must await analyses of a larger data set.

Goldberg et al. (1986) have examined the relationship between compressional wave velocity and porosity for logging data at Sites 612 and 613 and have shown that the oozes from Unit I and upper Unit II have velocities close to those predicted by simple models of fluid and unconnected particles (Wood, 1930). As velocities and depth increase, the velocity-porosity relationship trends more towards the traditional time average equations used in sedimentary rocks (Wyllie et al., 1958). The increase in attenuation (decrease in Q_p) seems to reflect the same sort of trend. At the seawater-sediment interface Q is that of water and is relatively large. As the ratio of sediment particles to seawater increases, so too does the attenuation. The sediments eventually lithify and will possess Q_p values of 50-100 based on results of laboratory determinations (Johnston et al., 1979). The results of this study suggest that there is a zone of minimum Q_p where some attenuation mechanism, such as frictional dissipation, is dominant. Eventually the profile of Q_p must again increase as increasing cementation of grains reduces the effects of the dominant mechanism.

Results of the inversion for V_s are less clear at this point in the study. Shear wave velocities exhibit the most variation in the interval of approximately 440 to 540m BSF at Site 613. This is also an interval of variability in V_p and electrical properties (Figure 5.). The reason for this variation in V_s may be either due to differential cementation or small scale changes in composition. There is some suggestion in samples from the core which were examined petrographically that there may be a segregation of cements along with the diagenetic change. Carbonate contents of individual samples from the core vary in the same manner as V_p and formation factor F although the mean composition of Unit III is essentially the same as Unit II (Wilkens et al., 1986). Relatively greater shear wave velocities may represent better cementation of the grains in discrete zones

or simply reflect a difference in the silica content of those zones. Further work with other logging properties as well as data from other sites will be required to adequately distinguish between these two possibilities.

ACKNOWLEDGEMENTS

This work was supported by the Full Waveform Acoustic Logging Consortium at M.I.T. and by the National Science Foundation under grant No. OCE-8408761. J.A. Meredith was supported by a Chevron Fellowship. R.H. Wilkens was supported by the Deep Sea Drilling Project while on Leg 95.

REFERENCES

Bouchon, M., and Aki, K., 1977, Discrete wave-number representation of seismic-source wave fields, Bull. Seis. Soc. Am., 67, 259-277.

Cheng, C.H., and Toksöz, M.N., 1981, Elastic wave propagation in a fluid-filled borehole and synthetic acoustic logs, Geophysics, 46, 1042-1053.

Cheng, C.H., Toksöz, M.N., and Willis, M.E., 1982, Determination of *in situ* attenuation from full waveform acoustic logs, J. Geophys. Res., 87, 5477-5484.

Goldberg, D.G., Moos, D., and Anderson, R.N., 1985, Attenuation changes due to diagenesis in marine sediments, Trans. SPWLA 26th Ann. Logging Symp., paper KK, June 17-20.

Goldberg, D.G., Wilkens, R., and Moos, D., 1986, Seismic modelling of diagenetic effects in Cenozoic marine sediments, Init. Repts. DSDP, 95, in press.

Johnston, D.H., Toksöz, M.N., and Timur, A., 1979, Attenuation of seismic waves in dry and saturated rocks: II. Mechanisms, Geophysics, 44, 691-711.

Leg 95 Scientific Party, 1984, DSDP Leg 95 adds data on the Atlantic margin, Geotimes, 29, 14-16.

Paillet, F., and Cheng, C.H., 1986, A numerical investigation of head waves and leaky modes in fluid-filled boreholes, Geophysics, in press.

Stephen, R.A., Pardo-Casas, F., and Cheng, C.H., 1985, Finite-difference synthetic acoustic logs, Geophysics, 50, 1588-1609.

Tsang, L., and Rader, D., 1979, Numerical evaluation of the transient acoustic waveform due to a point source in a fluid-filled borehole, Geophysics, 44, 1706-1720.

Wilkens, R.H., Schreiber, B.C., Caruso, L.Y., and Simmons, G., 1986, The effects of diagenesis on the microstructure of Eocene sediments bordering the Baltimore Canyon Trough, Init. Repts. DSDP, 95, in press.

Wood, A.B., A Textbook of Sound, 1930, G. Bell and Sons, London.

Wyllie, M.R.J., Gregory, A.R., Gardner, G.H.F., 1958, An experimental investigation of factors affecting elastic wave velocities in porous media, Geophysics, 23, 459-493.

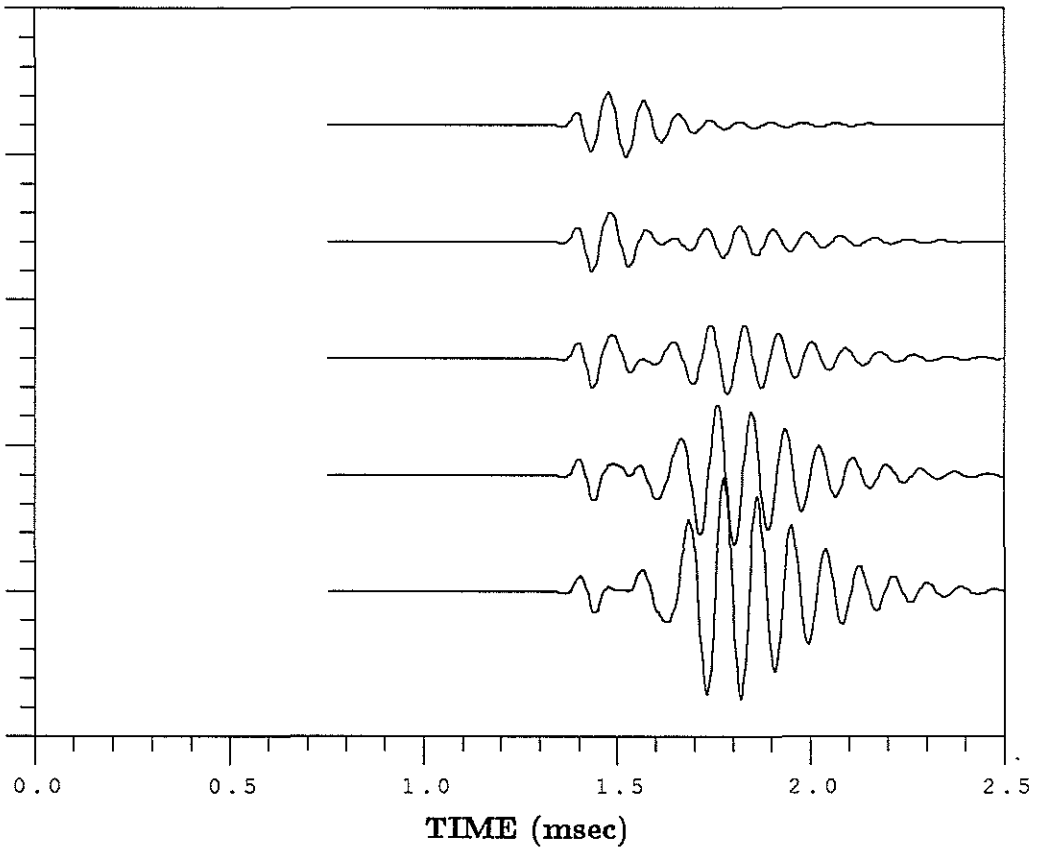

Figure 1: Synthetic microseismograms generated for varying Poisson's ratio and constant V_p. From top to bottom, the Poisson's ratios are: 0.321, 0.358, 0.385, 0.416, 0.441.

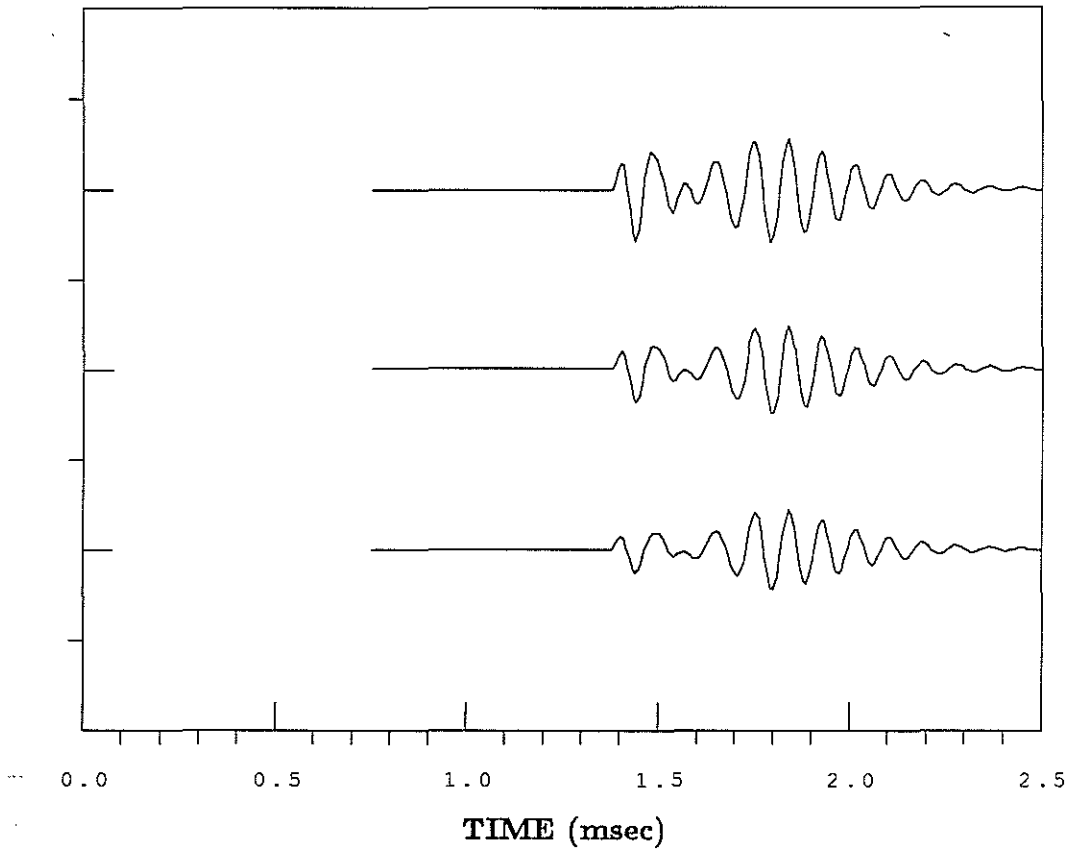

Figure 2: Synthetic microseismograms generated for varying Q_p. From top to bottom, the Q_p values are: 100, 50, 35.

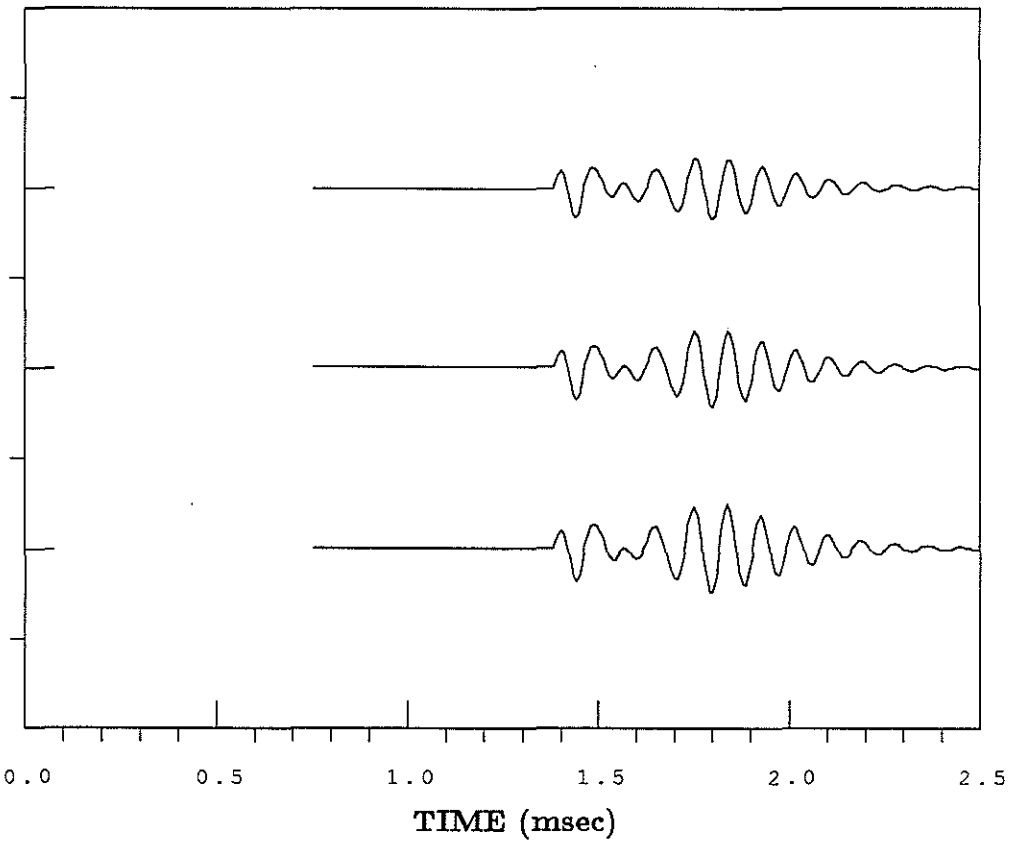

Figure 3: Synthetic microseismograms generated for varying Q_s. From top to bottom, the Q_s values are: 10, 20, 50.

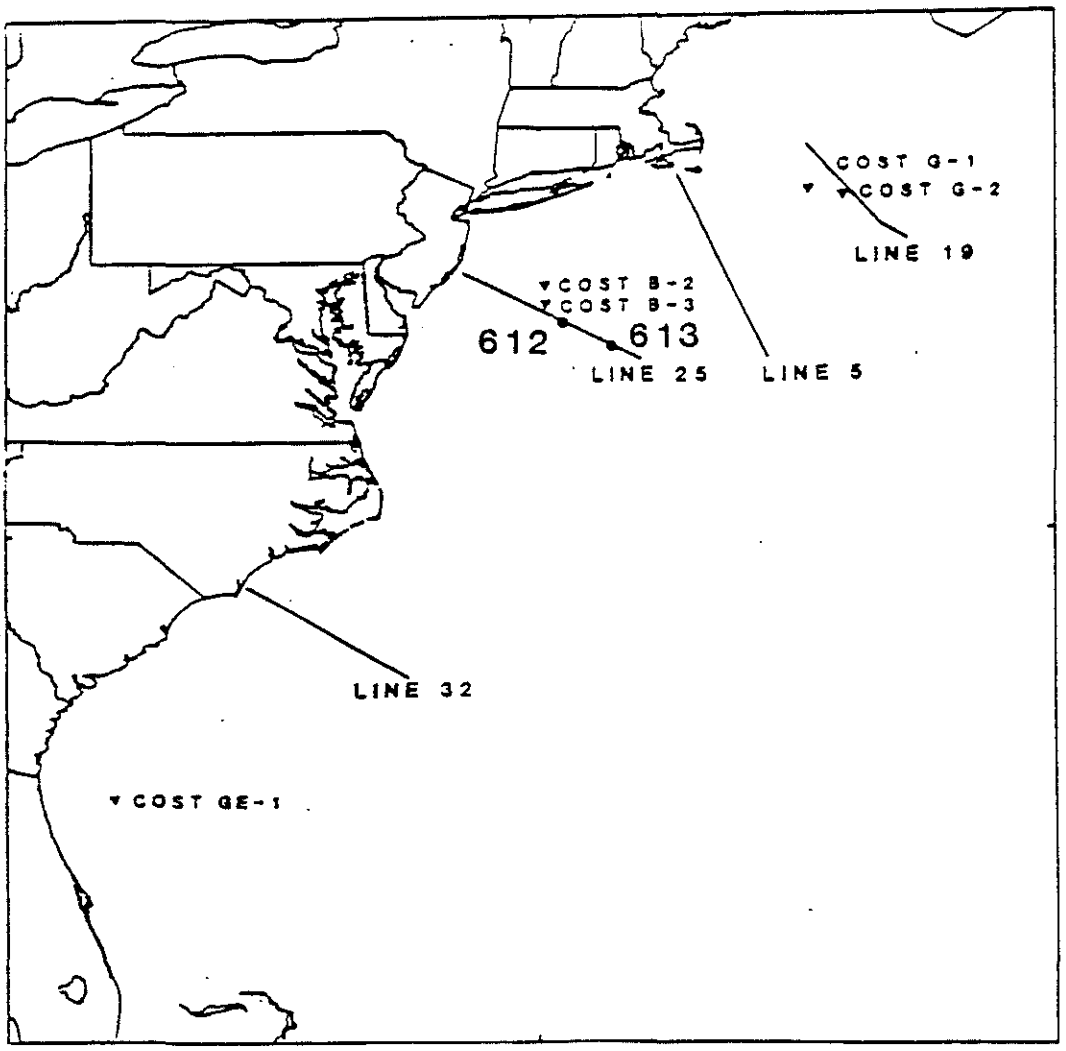

Figure 4: Map showing the locations of DSDP Sites 612 and 613. Sites were located on USGS multichannel seismic line 25, down slope from COST B2 and B3 test wells.

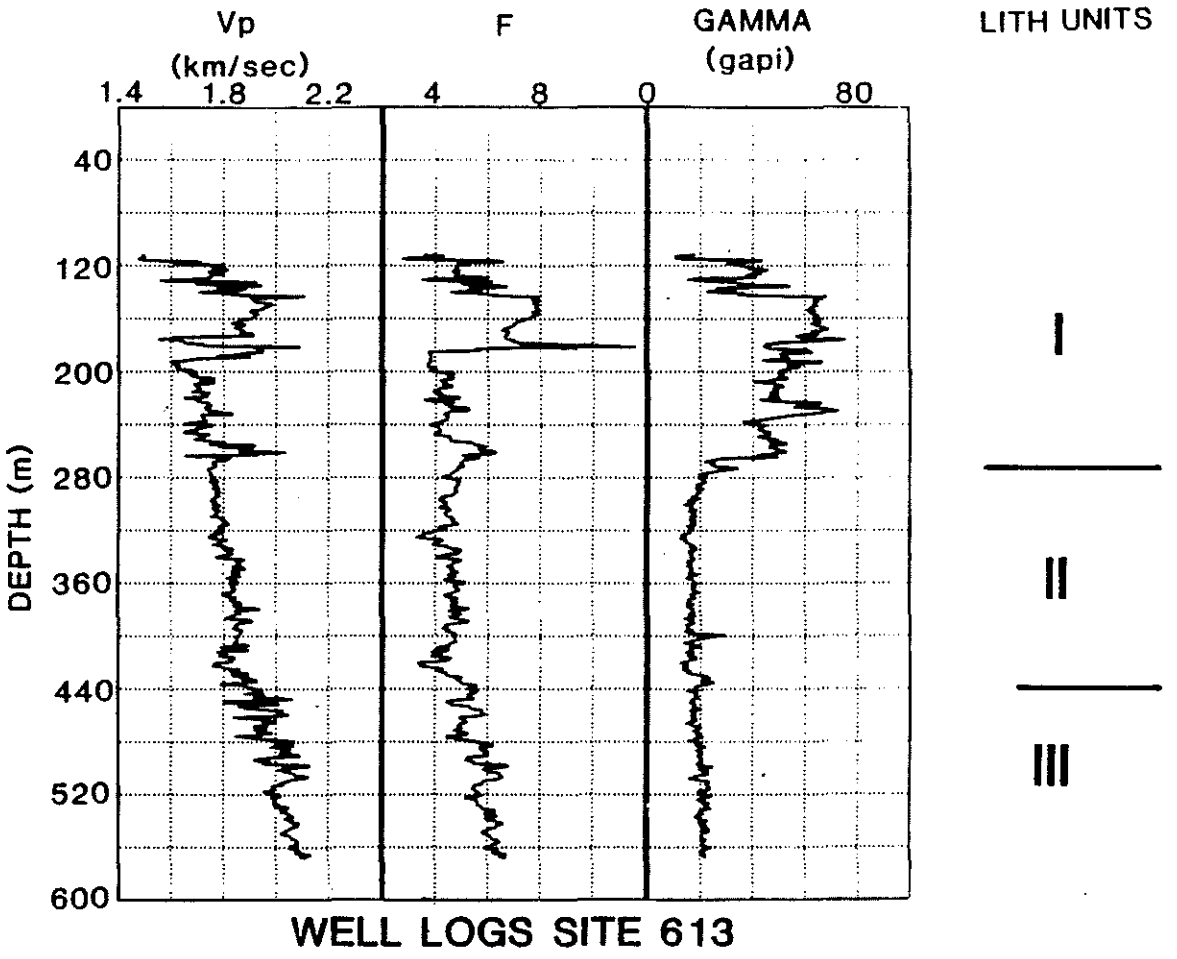

Figure 5: Well log data from DSDP Site 613. Formation factor (F) was calculated from resistivity log using salinity values of pore water samples taken during drilling. Depth is in meters below sea floor. Water depth was 2330m.

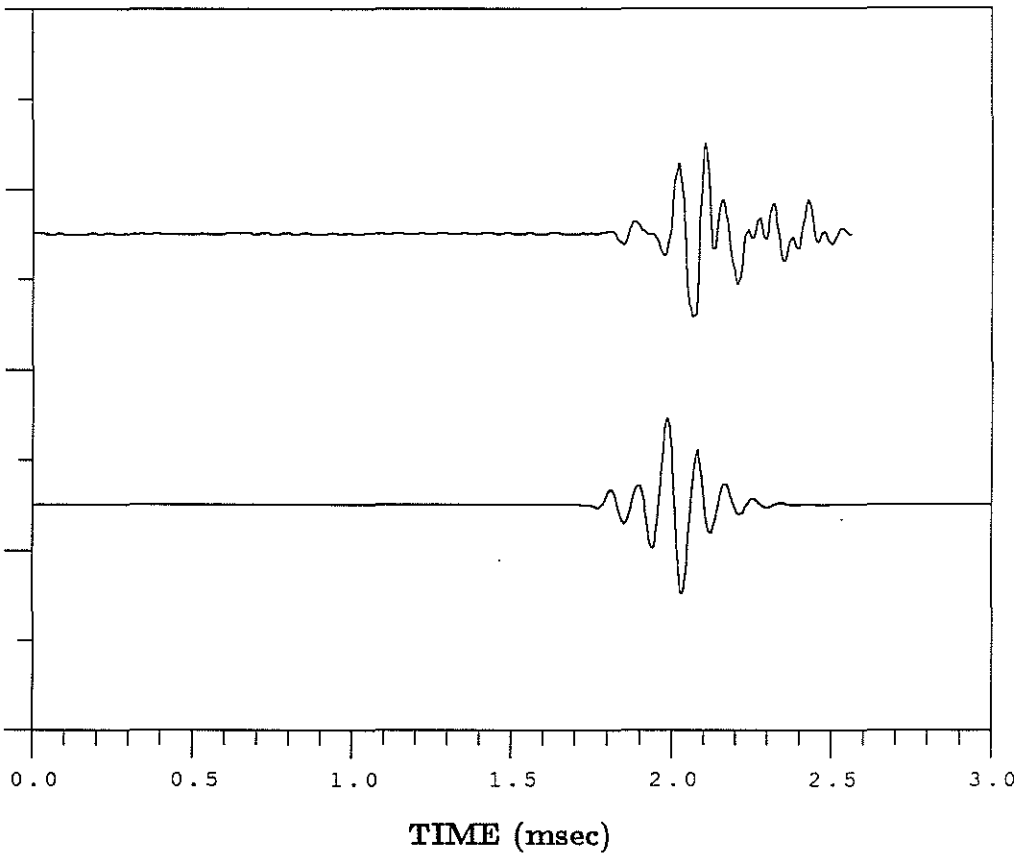

Figure 6: A comparison of the actual (top) and synthetic (bottom) full waveform acoustic log microseismogram at a depth of 200mBSF. The synthetic microseismogram was generated using the V_s and Q_p values obtained from the inversion of the actual microseismogram.

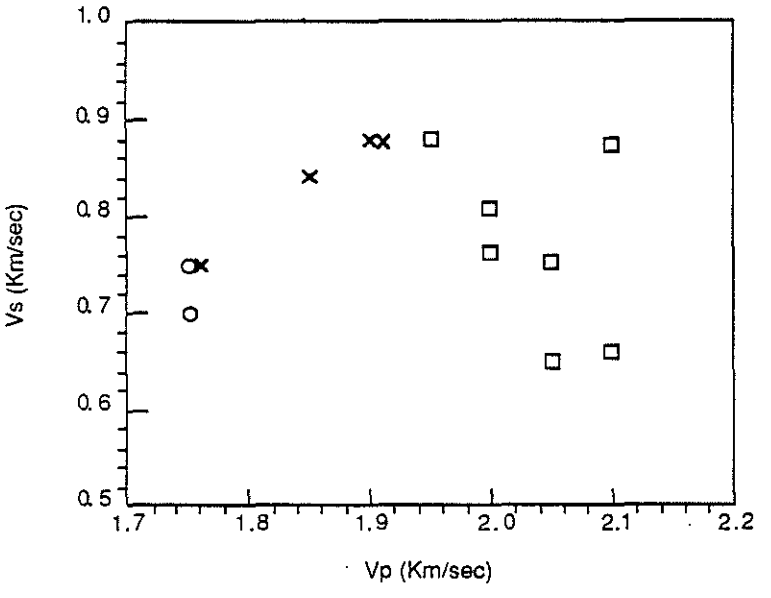

Figure 7: V_p plotted versus V_s from inversion results of thirteen Site 613 waveforms. Circles represent lithologic Unit I, crosses - Unit II, and squares - Unit III.

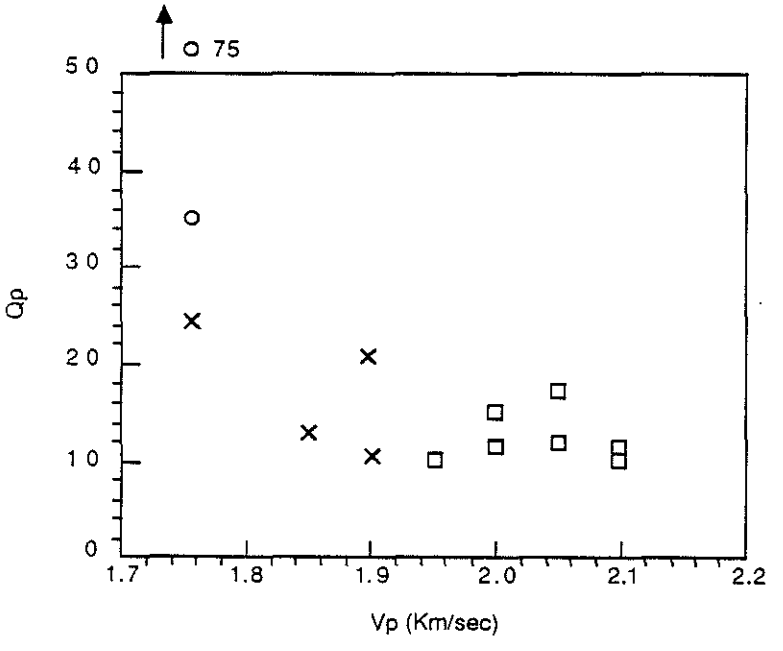

Figure 8: V_p plotted versus Q_p from inversion results of thirteen Site 613 waveforms. Circles represent lithologic Unit I, crosses - Unit II, squares - Unit III.